

DYNAMICS OF CHARGE COLLECTION FROM
ALPHA-PARTICLE TRACKS IN INTEGRATED CIRCUITS

C. M. Hsieh, P. C. Murley and R. R. O'Brien
IBM General Technology Division, East Fishkill
Hopewell Junction, New York 12533

Abstract

We studied the transient characteristics of charge collection from alpha-particle tracks in silicon devices. We have run computer calculations using the finite element method, in parallel with experimental work. When an alpha particle penetrates a pn-junction, the generated carriers drastically distort the junction field. After alpha particle penetration, the field, which was originally limited to the depletion region, extends far down into the bulk silicon along the length of the alpha-particle track and funnels a large number of carriers into the struck junction.

After less than one nanosecond, the field recovers to its position in the normal depletion layer, and, if the track is long enough, a residue of carriers is left to be transported by diffusion. The extent of this field funneling is a function of substrate concentration, bias voltage, and the alpha-particle energy.

Introduction

Since the recognition by May and Woods¹ that alpha particles from impurities in packaging materials can cause soft errors in some semiconductor memory chips, a number of papers have appeared on various aspects of the subject. Our purpose in this work is to develop a complete understanding of the mechanism whereby charge from an alpha track in silicon is collected at the surface. Specifically, we are interested in the relative roles of drift and diffusion in the process of charge collection.

A simplified model for the diffusion and collection of the charge generated along the track was treated numerically by Kirkpatrick.² For a uniform collecting surface, he calculated the carrier distribution that results from the diffusion of carriers generated by ionizing radiations. Although this work is useful in certain applications, his assumption that the transport mechanism is pure diffusion neglects one key ingredient. A paper using the Monte Carlo technique³ also makes a similar simplifying assumption. We have found through this experimental and numerical study that when an alpha particle hits a junction, the field-enhanced funneling below the original depletion layer plays an important role in the charge collection process.

Computer Simulation

In our computer calculations we used finite element techniques. These methods have been extensively employed in device design and analysis.⁴ They can provide simultaneous solutions of Poisson's equation and the hole-and-electron continuity equations. To model the alpha particle strike, we calculated the initial potential and carrier distribution in a device before the alpha particle struck.

The alpha particle strike was then simulated by introducing a properly varying density of hole-electron pairs along the track of the particle. Next, we ran a transient calculation with this modified initial condition. Thus, for the problem of the collection of carriers from an alpha particle track, we found a self-consistent solution that included both the charges arising from the subsequent motion of the holes

and electrons in the track and the effect of these charges on the motion of all carriers.

The most important of these effects is that which we call field funneling. If the generated carriers cross a high field region such as the depletion region around a pn-junction, the presence of the carriers distorts the associated electric field and causes it to spread down along the track into previously field-free regions. The field will cause carriers in the track to be collected rapidly by drift rather than slowly by diffusion. In less than a nanosecond, the generated carrier density near the junction becomes comparable to the substrate doping, and the disturbed field relaxes back to its original position as the junction re-establishes itself. Hence, the extent of this drift is strongly dependent on the impurity concentration of the silicon substrate. In the calculations, carrier transport was considered in three dimensions as well as in two.⁵

Results of the calculations are shown in the following figures. Figure 1(a) and 1(b) are the plots of the potential and electron density distributions 0.1 ns after the alpha particle strikes for 14 ohm-cm. The region of potential change is no longer confined to a small area at the top of the structure near the pn-junction but has spread down along the track into the substrate. Figures 2(a) and 2(b) show the potential and electron density distributions at 0.5 ns as they are relaxing back towards their original locations. Figure 3 shows the transient current at the collection node. Figure 4 shows the calculated charge collection as a function of time. Two distinct time constants were observed.

Experimental Results

To verify the computed results, we made many measurements of the various charge collection characteristics due to alpha-particle strikes on silicon devices. Since the number of parameters (bias voltage, alpha-particle energy, angle of incidence, collector area, etc.) that we can vary in this study is large, a large amount of data was gathered. Rather than attempt to describe all our experimental results, we will present only some of our important findings. Details of the results will be published in a full-length article elsewhere.

In this paper, we restricted ourselves to a discussion under the following conditions: the devices were large in area (480 μm by 1000 μm , had shallow n+ diffusions on 2 and 14 ohm-cm substrates, and an alpha source of Am-241 was used for testing -- primarily at normal incidence to the junction.

We measured the collection time through a high-impedance probe and displayed it on a high frequency (GHz) real-time oscilloscope. This measurement system was calibrated by using a short risetime (70 ps) pulse generator. It has proved to be fast enough to measure the time profile of charge collection. Figure 5 shows a typical photographic result of the direct measurement of the charge collection time profile. Two distinct time constants appear in this single-shot voltage waveform. First there occurs a very fast drop as electrons are collected, and then an abrupt leveling off to a slow decline. Time scale expansion of

the scope as shown in Figure 6 indicates that the fast drop part takes no more than 1.3 ns. During this initial time interval, the overwhelming part of the carriers collected is contributed by field-enhanced funneling. A small number of carriers may also be collected by diffusion during this time period. For simplicity, we refer to this fast drop part of the charge collected as the drift component. After this initial time of funneling, the field collapses back to its original configuration. A residue of carriers, which has been pulled up close to the junction, remains to be transported by diffusion, and a portion of it is collected by the n⁺ region. This long time-constant part of the charge collected is identified as the diffusion component.

For alphas of low energy, the collection efficiency is higher because of the Bragg peak effect. Figure 7 shows the collection time profile for an alpha energy of 3 MeV. Its drift component is higher than that of a 4.3 MeV, and the charge collection is almost completed by the drift process alone.

We took hundreds of photographs under various conditions and measured the amplitudes of both the overall collection and the drift component. Since it is difficult to accurately determine the actual capacitance of the test node in the case of a high speed pulse, we measured the actual packet of the charge collected by using another system. This measurement is in addition to deriving the charge magnitude from the voltage of the time measurements.

The total charge collected was measured with a charge-sensitive preamplifier and a spectroscopic amplifier and was analyzed with a multichannel analyzer. This system was calibrated with silicon-surface-barrier detectors. After accurately obtaining the total charge, we determined the drift component from the amplitude ratio of the single-shot voltage waveform taken at time measurements. As an example, for an alpha energy of 4.3 MeV and a bias voltage of 8.0 volts, the diode on the 14 ohm-cm substrate collected 168 fC of charge, and 55% of that was drift component; the same size diode on a 2 ohm-cm substrate collected only 130 fC, and only 25% of that was drift component.

Figure 8 shows the collected charge as a function of alpha particle energy. Because of the large collecting area, the total charge collected increased with the alpha-particle energy. However, the drift component decreased at high alpha energy. This was due to the non-uniform carrier density generated along the track. The higher densities occurred at the end of the track. When the depletion region of the pn junction is distorted, the extended electric field keeps driving the carriers to the n⁺ region until the carrier density near the junction is about equal to the substrate doping and the depletion layer is re-established. Therefore, the drift component of collection of the high-resistivity substrate was observed to be much larger than that of the low-resistivity one.

The bias voltage sensitivities were also measured. As the bias voltage increases, the drift component increases much faster than the total charge collection. This situation is much more prominent for high-resistivity than for low-resistivity substrates, as shown in Figure 9.

From the preceding, it is evident that the drift component includes much more charge than the charge released within the original depletion layer. The dash-dot lines shown in Figure 9 represent the calculated equivalent charge that would be generated within the original depletion layer if the junction field had not been distorted after the alpha-particle strike.

From the measured charge in the drift component, we can calculate the equivalent depth of collection using the ionization density distribution along the track. Figure 10 shows the equivalent funneling depth as a function of the substrate doping concentration. As an example, the funneling effect is equivalent to the total collection of all charge for a distance of about 10 μ m beyond the original depletion layer for a device on a 14 ohm-cm substrate, which is biased at 15 volts and struck by a 4.3 MeV alpha particle.

For a more direct comparison of the calculations and measurements, we show in Figure 11 an explicit comparison of the collection time profile for theory and experiment. The agreement is excellent.

Implication for Integrated Circuit Reliability

Collecting a large amount of charge in a short time is detrimental to circuit function. The drift component is relatively independent of collecting area, while the diffusion component is a strong function of collecting area. Therefore, the drift component, which is enhanced by the funneling effect, becomes the dominant factor for soft error rate (SER) due to charge collection from alpha-particle tracks in high-density VLSI. For current 64K RAMs, the floating time, which is the time window in which the bit lines and the sense amplifiers are susceptible to being upset by alpha-particles, may be only 20 ns or so for each cycle. Therefore, it will make great differences in the calculations of soft error rates whether the charge collection from beyond the depletion region is by the slow process of diffusion alone or by the much faster process of field-funneling plus diffusion.

A struck node gets most of the charge collected. The charge-sharing effect due to diffusion is small for lowly-doped substrates. Therefore, the SER will not be reduced by decreasing the target and collection areas as in the case of making a denser array. The effectiveness of "folded bit lines" in reducing the SER appears to be very limited also. However, higher doping concentrations in the substrate will result in a lower SER.

Conclusions

The funneling effect that we have described, was observed in computer calculations and verified by experiments. After an alpha penetration, the depletion field extends far down into the bulk silicon and quickly funnels a large number of carriers into the struck junction. The funneling component of charge collection was found to be a strong function of the substrate doping concentration. In collecting charge, lowly-doped substrates are much more sensitive to bias voltage variations than highly-doped substrates.

Acknowledgments

The authors would like to express their appreciation to C. S. Chang, E. L. Boyd, D. B. Eardley and W. E. Mutter for many useful discussions, to F. L. Carbalan, C. G. Majtenyi and B. Masters for their co-operation in the experiments, and to E. M. Buturia and P. E. Cottrell for cooperation in the calculations.

References

1. T. C. May and M. H. Woods, IEEE Trans. Electron Dev., Vol. ED-26, pp. 2-9, (Jan 1979).
2. S. Kirkpatrick, IEEE Trans. Electron Dev., Vol. ED-26, pp. 1742-1753, (Nov 1979).
3. G. Sai-Halasz and M. R. Wordman, IEEE Trans. Electron Dev. Letters, Vol. EDL-1, No. 10, pp. 211-213, (Oct 1980).
4. P. E. Cottell and E. M. Buturla, Proc. NASECODE I Conf., pp. 31-64, (June 1979).
5. C. M. Hsieh, P. C. Murley and R. R. O'Brien, to be published at IEEE Trans. Electron Dev. Letters, (Apr 1981).

Equipotential Lines Electron Concentration

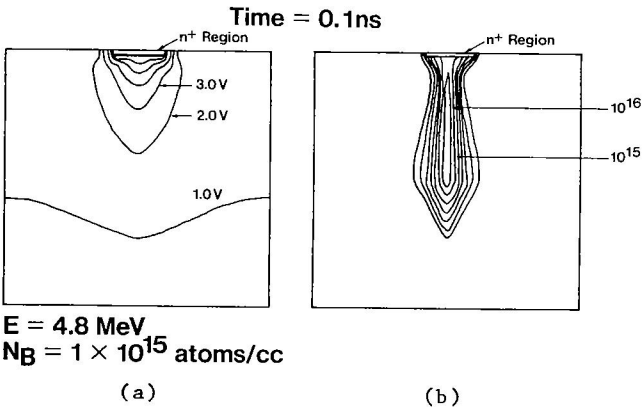


Fig. 1 Contour plot of (a) the potential distribution and (b) the electron concentration distribution at 0.1 ns. In (a) each contour interval is 1.0 volt. The alpha-particle energy is 4.8 MeV, the bias voltage 8.0 volts and the substrate resistivity 14 ohm-cm.

Equipotential Lines Electron Concentration

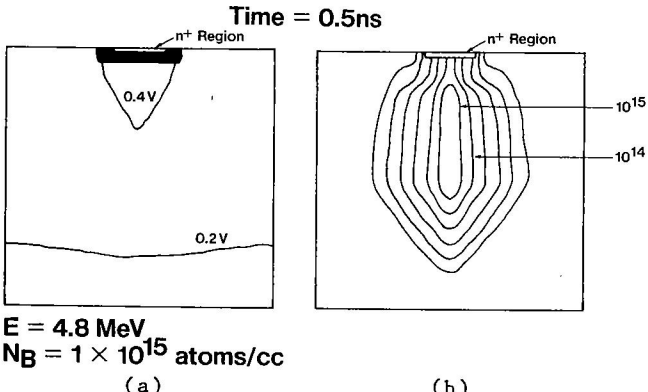


Fig. 2 Contour plot of (a) the potential distribution and (b) He electron concentration distribution at 0.5 ns. In (a) each contour interval is 0.2 volt. The alpha-particle energy is 4.8 MeV, the bias voltage 8.0 volts and the substrate resistivity 14 ohm-cm.

Computed Transient Current

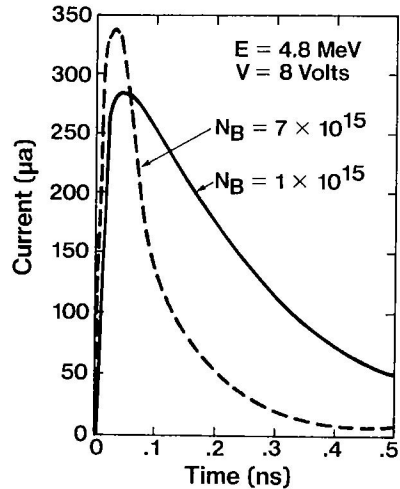


Fig. 3 Calculated transient current at a collection node.

Computer Simulation Results

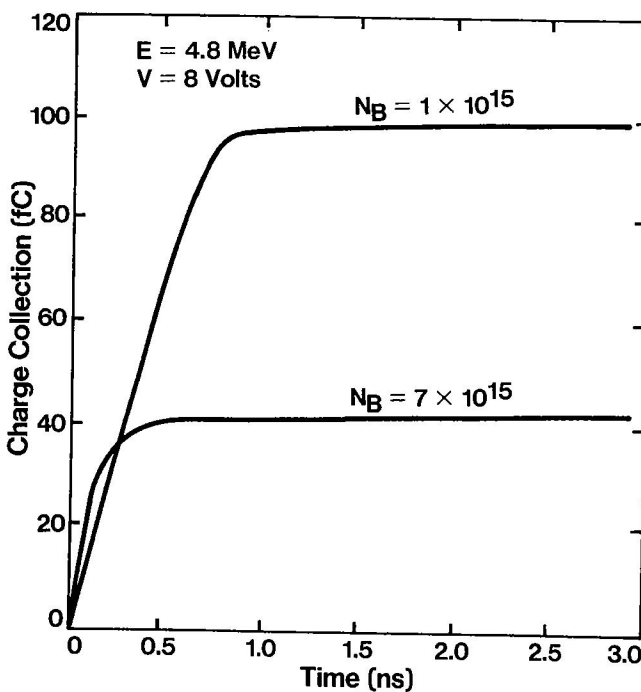


Fig. 4 Calculated charge collection as a function of time.

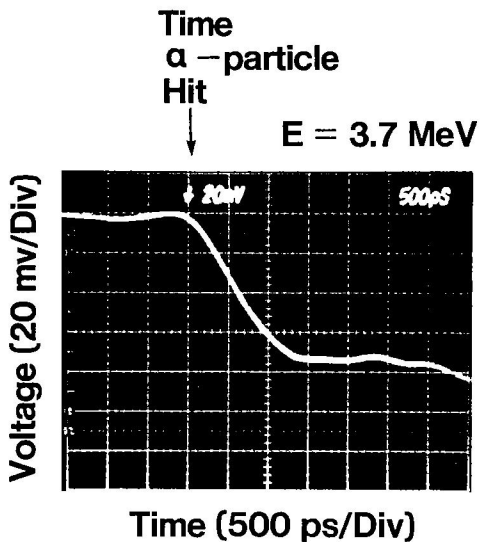
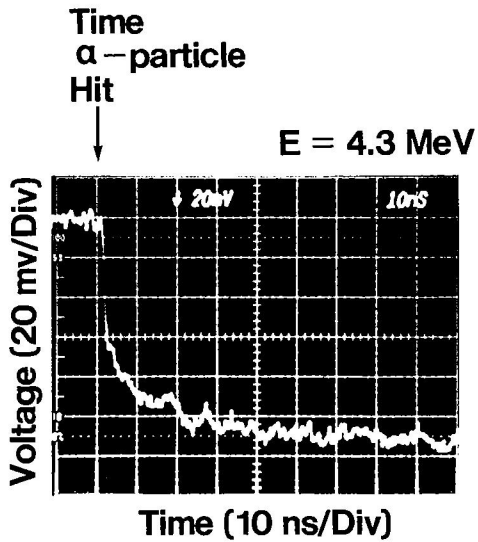


Fig. 6 Collection transient curve at 3.7 MeV and 8.0 volts bias. The time scale is 500 ps per division.

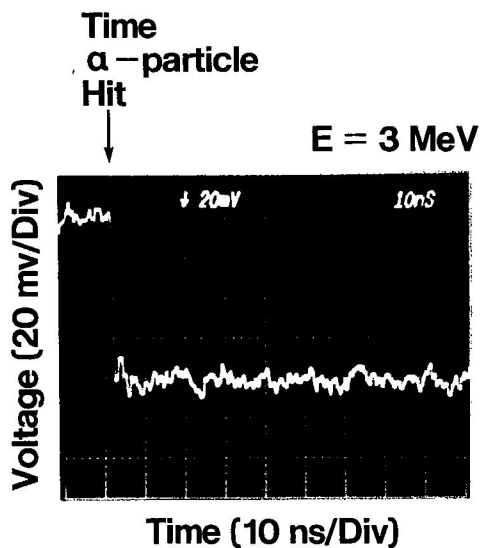


Fig. 5 A typical single-shot voltage waveform from the collection time measurements. The alpha-particle energy is 4.3 MeV, the bias voltage 8.0 volts, and the substrate resistivity 14 ohm-cm.

Charge Collection as a Function of α Energy

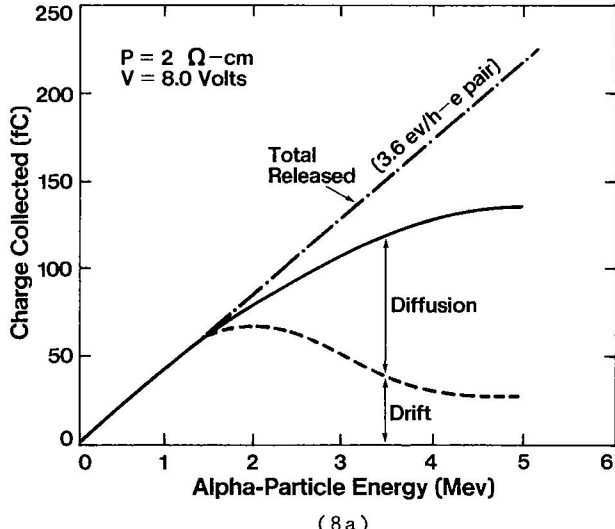


Fig. 8 The charge collected as a function of alpha-particle energy for a substrate with a resistivity of (a) 2 ohm-cm and (b) 14 ohm-cm, with a bias voltage of 8.0 volts. The measurements shown are for the total charge collected (solid line) and for the drift component (dotted line).

Charge Collection as a Function of α Energy

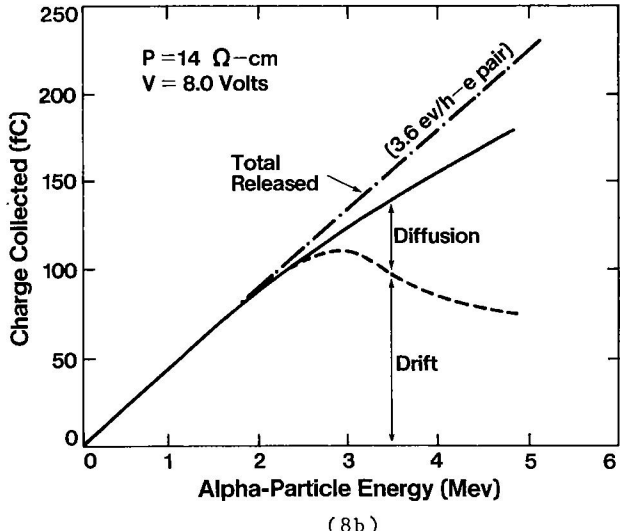
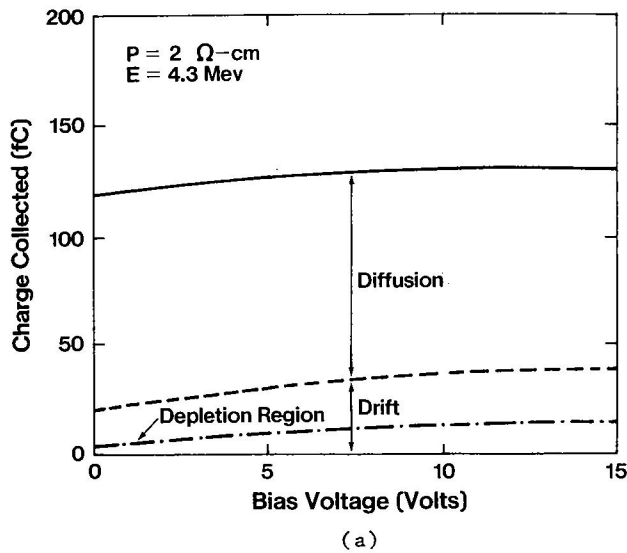


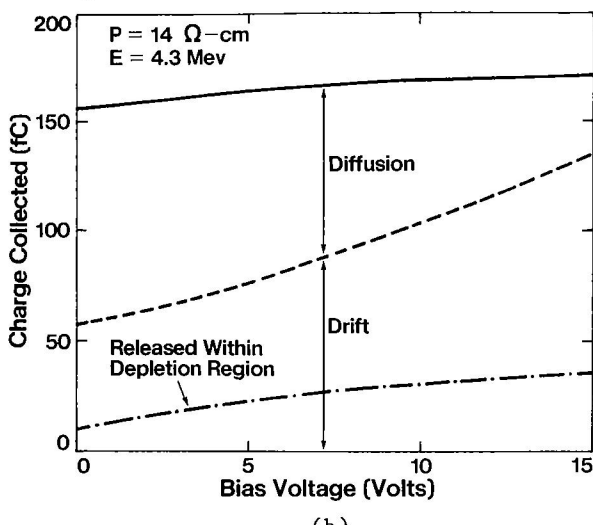
Fig. 7 Collection time profile for an alpha energy 3 MeV. The charge collection is almost entirely by the drift process alone.

Voltage Sensitivity



(a)

Voltage Sensitivity



(b)

Fig. 9 The charge collected as a function of bias voltage for a substrate with a resistivity of (a) $2 \Omega\text{-cm}$ and (b) $14 \Omega\text{-cm}$, with an alpha-particle energy of 4.3 MeV . The measurements shown are for the total charge collected (solid line) and for the drift component (dotted line). The dash-dot lines are the calculated equivalent charge generated within the original depletion layer before the field distortion.

Funneling Depth

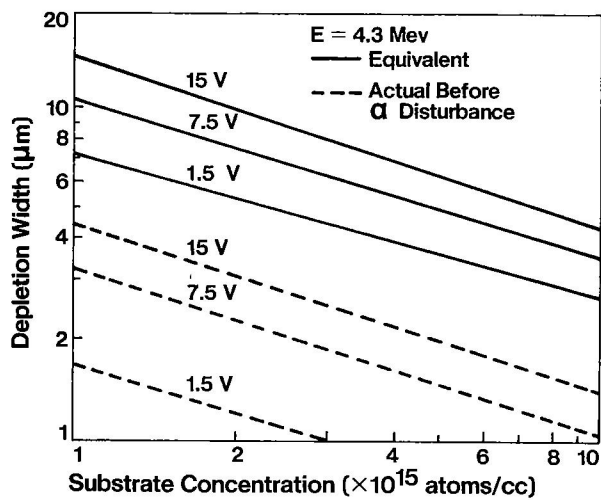


Fig. 10 The equivalent funneling depth as a function of substrate doping concentration.

Calculation vs Experimental Results

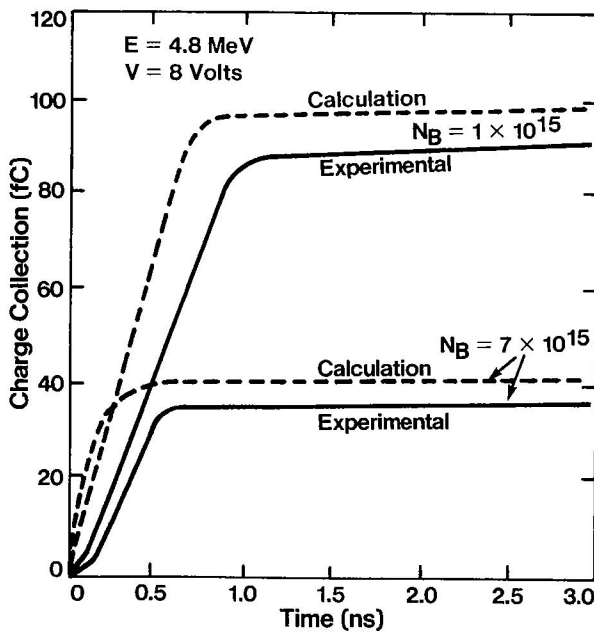


Fig. 11 A comparison of the calculated and experimental results.